SYSTEMATIC APPROACH TO OPTIMUM CHIP PULSE SHAPE DESIGN

Felix Antreich[(1)], Josef A. Nossek[(2)], Jean-Luc Issler[(3)]

(1) German Aerospace Center (DLR), Institute for Communications and Navigation, 82234 Wessling, Germany,

(2) Institute for Circuit Theory and Signal Processing, Munich University of Technology (TUM), 80333 Munich, Germany,

(3) Transmission Techniques and Signal Processing Department, Centre National d'Etudes Spatiales (CNES), 31401 Toulouse cedex 9, France,

E-mai: (1) felix.antreich@dlr.de, (2) nossek@nws.ei.tum.de, (3) jean-luc.issler@cnes.fr .

ABSTRACT

In this work we establish a systematic approach to design optimum chip pulse shapes for DS-CDMA systems which are absolutely bandlimited, whose energy is mainly concentrated in one chip duration, and that minimize the Cramer-Rao lower bound for the time-delay. The proposed methodology makes it possible to formulate the problem of designing optimum chip pulse shapes in terms of achieving a trade-off between synchronization accuracy and acquisition and tracking robustness as an optimization problem. This methodology is based on the prolate spheroidal wave functions (PSWF), which enable to transform the primal variational problem into the dual, tractable parametric optimization problem. This work shows the interesting capabilities of the presented signal design approach for DS-CDMA systems. Two design examples for signal design are shown for global navigation satellite systems (GNSS) considering different requirements and constraints.

1. INTRODUCTION

Besides the design of the applied pseudo noise (PN) binary sequences with regards to cross-correlation properties and jamming margin [1] , the design of the chip pulse shape for these PN sequences also needs to be considered in order to shape the autocorrelation function and to control the bandwidth occupancy of the signal. For precise synchronization the important trade-off between achievable synchronization accuracy, acquisition and tracking robustness needs to be achieved. Especially in the framework of global navigation satellite systems (GNSS), the signal shall also provide robustness against tracking errors induced by multipath signals [2]. Furthermore, various additional constraints regarding signal generation and spectral separation to other non-interoperable signals in the same band if any need to be considered as well. Thus, there is great demand for a systematic approach to signal design in order to consider all these different requirements and constraints jointly.

In this work we establish a systematic approach to design optimum chip pulse shapes for DS-CDMA systems which are absolutely bandlimited, whose energy mainly is concen-trated in one chip duration, and that minimize the Cramer-Rao lower bound (CRLB) for the time-delay. The proposed methodology makes it possible to formulate the problem of designing optimum chip pulse shapes in terms of achieving a trade-off between synchronization accuracy and acquisition and tracking robustness as a tractable optimization problem. Previous work by the authors established the basic methodology and showed that this approach is very promising and advantageous [3, 4]. In this work the proposed approach will be extended and further details will be explored. Additional constraints are introduced to the optimization problem in order to ensure a smooth cut-off of the power spectrum at the edges of the signal band and on the other hand to limit the spectral separation coefficient (SSC) [5] between the newly designed signals and other non-interoperable signals which are present in the same band. This methodology is based on the prolate spheroidal wave functions (PSWF) [6, 7], which enable to transform the primal variational problem into the dual, tractable parametric optimization problem. Related work about using the PSWF for pulse chip shape design considering various constraints was reported in [8, 9, 10], but here time limited pulses were favoured, different cost functions were applied than the CRLB and the important trade-off between synchronization accuracy and acquisition and tracking was not considered.

The presented systematic approach to DS-CDMA signal design is a powerful methodology to accomplish a signal design which enables to be in full control of all the design parameters. The derived low complexity optimization problem can be solved easily and reliably. Especially, for GNSS signal design this methodology enables to achieve the trade-off between achievable synchronization accuracy and acquisition and tracking while considering additional constraints regarding signal generation and spectral separation.

2. SYSTEM MODEL

We assume coherent downconversion of the radio frequency signal to baseband. The received DS-CDMA baseband navi-

gation signal of one satellite is given by

$$y(t) = \sqrt{P}\, c(t - \tau) + n(t), \qquad (1)$$

where P denotes the signal power, $c(t)$ is the pseudo noise (PN) binary sequence, τ is the time delay of the user, and $n(t)$ is white Gaussian noise with power spectral density of $N_0/2$. Thus, the PN sequence is given by

$$c(t) = \sum_{k=0}^{N_c} c_k\, \delta(t - kT_c) * p(t), \qquad (2)$$

where $p(t)$ denotes the chip pulse shape, and $c_k \in \{-1, 1\}$ are the code bits of the PN sequence.

In order to perform precise synchronization in a navigation receiver the delay τ needs to be estimated with high accuracy. The variance of the delay estimation error σ_τ^2 of any unbiased estimator is lower bounded by the Cramer-Rao lower bound (CRLB). The CRLB can be given [11]

$$\sigma_\tau^2 \geq \frac{B_n}{C/N_0\, 8\pi^2} \frac{\int_{-\infty}^{\infty} |P(f)|^2\, df}{\int_{-\infty}^{\infty} f^2\, |P(f)|^2\, df}, \qquad (3)$$

where B_n denotes the (two-sided) noise bandwidth [12, 13] of the generic estimator, $P(f)$ is the Fourier transform of the chip pulse shape $p(t)$, and C/N_0 denotes the carrier-to-noise density ratio of the received signal. For long PN sequences the autocorrelation function $R(\varepsilon)$ can be approximated as

$$R(\varepsilon) \approx \int_{-\infty}^{\infty} p(t)p(t - \varepsilon)\, dt = \int_{-\infty}^{\infty} |P(f)|^2 e^{j2\pi f \varepsilon}\, df. \quad (4)$$

3. SIGNAL DESIGN APPROACH

In the following we will outline a systematic approach to optimum chip pulse shape design in order to design signals with defined properties. Our goal is to design chip pulse shapes $p(t)$ which are absolutely bandlimited to $[-B, B]$, whose energy mainly is concentrated within $[-T_c/2, T_c/2]$, and which accomplish a trade-off between synchronization accuracy on the one hand and tracking and acquisition robustness on the other hand. Synchronization accuracy is given by the CRLB defined in (3). Thus, we choose the CRLB as our cost function which will be minimized. The minimization is subject to the constraint

$$\int_{-\infty}^{\infty} |P(f)|^2\, df = 1. \qquad (5)$$

Minimizing the CRLB subject to (5) leads to maximizing $\int_{-\infty}^{\infty} f^2\, |P(f)|^2 df$, which denotes the second moment of the power spectrum $|P(f)|^2$. This is equal to maximizing the curvature of the autocorrelation function $R(\varepsilon)$ at $\varepsilon = 0$ as from basic theorems of the Fourier transform and (4) $\int_{-\infty}^{\infty} f^2\, |P(f)|^2 df \approx -\frac{1}{4\pi^2} \left.\frac{d^2\, R(\varepsilon)}{d\,\varepsilon^2}\right|_{\varepsilon=0}$ [14].

Tracking and acquisition robustness is addressed by limiting the side extrema of the autocorrelation function $R(\varepsilon)$ besides the global extremum at $\varepsilon = 0$. This can be defined as an additional constraint:

$$\underset{i \in \mathbb{N}}{\forall}\, |\nu_i| \leq \kappa, \qquad (6)$$

where ν_i denote the value of $R(\varepsilon)$ at the local extrema besides the global maximum of $R(\varepsilon)$ for $\varepsilon = 0$. Thus, we limit the absolute value of the local extrema of $R(\varepsilon)$ to $\kappa \in [0, 1]$. The shaping coefficient κ quantifies the trade-off between synchronization accuracy and tracking and acquisition robustness.

Furthermore, it is desirable to ensure a smooth cut-off of the power spectrum $|P(f)|^2$ at $f = \pm B$. We define this as a constraint of our optimization problem:

$$|P(\pm B)|^2 \leq \gamma, \qquad (7)$$

whereas $\gamma \in \mathbb{R}^+$ denotes the upper bound for the cut-off of $|P(f)|^2$ at $f = \pm B$.

In GNSS signal design the spectral separation between non-interoperable signals in the same band plays an important role. The spectral separation of two signals can be for example quantified by the spectral separation coefficient (SSC) [5],

$$SSC = \int_{-\infty}^{\infty} \Phi_1(f)\, \Phi_2(f)\, df, \qquad (8)$$

where $\Phi_1(f)$ and $\Phi_2(f)$ denote the power spectral density of the two signals respectively. We now can include another constraint to our optimization problem. We can give an upper bound for the SSC in dB/Hz between the new designed signal and a certain non-interoperable signal in the same band:

$$\int_{-\infty}^{\infty} |P(f)|^2\, \Phi(f) df \leq SSC. \qquad (9)$$

3.1. Prolate Spheroidal Wave Functions (PSWF)

Whereas the resulting optimization problem is not tractable it is converted to an equivalent discrete formulation with reduced dimensions. This will be achieved by expanding the chip pulse shape $p(t)$ of a PN sequence using an adequate set of orthogonal basis functions. This approach transforms the apparent variational problem into a parametric optimization problem solving for the expansion coefficients that minimize the cost function. Special functions known as the prolate spheroidal wave functions (PSWF) are particularly well suited to form a set of basis functions [6]. They have the very interesting property of being orthogonal over two different intervals.

For any $B > 0$ and $T_c > 0$ the PSWF form an infinite set of real functions $\psi_0(\varrho, t), \psi_1(\varrho, t), \psi_2(\varrho, t), \ldots$ with associated real positive eigenvalues $\lambda_0(\varrho) > \lambda_1(\varrho) > \lambda_2(\varrho), \ldots$.

The ψ_m and λ_m are functions of the normalized time-bandwidth product $2\varrho = 2\pi T_c B$. The $\psi_m(\varrho, t)$ are bandlimited to $[-B, B]$ and form a complete and orthonormal set of functions [6]:

$$\int_{-\infty}^{\infty} \psi_m(\varrho, t)\, \psi_n(\varrho, t)\, dt = \left\{ \begin{array}{ll} 1, & m = n \\ 0, & m \neq n \end{array} \right. . \qquad (10)$$

They also form a complete and orthogonal set in the interval $[-T_c/2, T_c/2]$ [6]:

$$\int_{-T_c/2}^{T_c/2} \psi_m(\varrho, t)\, \psi_n(\varrho, t)\, dt = \left\{ \begin{array}{ll} \lambda_m(\varrho), & m = n \\ 0, & m \neq n \end{array} \right. . \qquad (11)$$

The PSWF are solutions of the integral equation [6]

$$\lambda_m\, \psi_m(\varrho, t) = \int_{-T_c/2}^{T_c/2} \frac{\sin(2\pi B(t-s))}{\pi(t-s)}\, \psi_m(\varrho, s)\, ds. \qquad (12)$$

The Fourier transform $\Psi_m(\varrho, f)$ of $\psi_m(\varrho, t)$ can be expressed in terms of $\psi_m(\varrho, t)$. Following [6, 15] we get

$$\Psi_m(\varrho, f) = \left\{ \begin{array}{ll} (-j)^m \sqrt{\frac{T_c}{\lambda_m\, 2B}}\, \psi_m(\varrho, f\frac{T_c/2}{B}) & \text{for } |f| \leq B \\ 0 & \text{else} \end{array} \right. \qquad (13)$$

Applying Parsival's theorem to (10) we get

$$\int_{-\infty}^{\infty} \Psi_m(\varrho, f)\, \Psi_n^*(\varrho, f)\, df = \left\{ \begin{array}{ll} 1, & m = n \\ 0, & m \neq n \end{array} \right. . \qquad (14)$$

The $\psi_m(\varrho, t)$ are real, even for m even and odd for m odd. Their Fourier transform $\Psi_m(\varrho, f)$ is real and even for m even and imaginary and odd for m odd. For the generation of the PSWF we followed [6, 16, 17].

Finally, we propose the expansion

$$p(t) = \sum_{m=0}^{\infty} \alpha_m \psi_m(\varrho, t), \qquad (15)$$

where $\{\alpha_m\}_{m=0}^{\infty}$ are the expansion coefficients. We now can transform the primal variational problem into a parametric optimization problem by setting $P(f) = \sum_{m=0}^{\infty} \alpha_m \Psi_m(\varrho, f)$.

3.2. Optimization Problem

The resulting parametric optimization problem now needs to be reduced in its complexity in order to make it tractable. The very interesting property of the PSWF of being orthogonal over two different intervals enables us to perform the following reduction of the optimization problem.

In the following we will restrict ourself to the case $\varrho = \pi$. From (10) and (11), a small value of λ_m implies that $\psi_m(\varrho, t)$ will have most of its energy outside $[-T_c/2, T_c/2]$, whereas a value of λ_m near 1 implies that $\psi_m(t)$ contains most of its energy within $[-T_c/2, T_c/2]$. For a fixed value of ϱ the λ_m

fall off to zero rapidly with increasing m once m has exceeded $\frac{2}{\pi}\varrho$. For the case $\varrho = \pi$ it is sufficient to use $m = 0, \ldots, M$ with $M = 5$. Thus, we can formulate the resulting parametric optimization problem:

$$\{\alpha_m^*\}_{m=0}^{M} = \underset{\{\alpha_m\}_{m=0}^{M}}{\arg\min} \left\{ \frac{\int_{-\infty}^{\infty} (\sum_{m=0}^{M} \alpha_m \Psi_m(\varrho, f))^2\, df}{\int_{-\infty}^{\infty} f^2\, (\sum_{m=0}^{M} \alpha_m \Psi_m(\varrho, f))^2\, df} \right\} \qquad (16)$$

subject to

$$\int_{-\infty}^{\infty} \left(\sum_{m=0}^{M} \alpha_m \Psi_m(\varrho, f) \right)^2 df = 1, \qquad (17)$$

$$\underset{i \in \mathbb{N}}{\forall}\ |\nu_i| \leq \kappa, \qquad (18)$$

$$\left(\sum_{m=0}^{M} \alpha_m \Psi_m(\varrho, \pm B) \right)^2 \leq \gamma, \qquad (19)$$

$$\int_{-\infty}^{\infty} \left| \sum_{m=0}^{M} \alpha_m\, \Psi_m(\varrho, f) \right|^2 \Phi(f) df \leq SSC. \qquad (20)$$

4. RESULTS

In order to derive chip pulse shapes $p(t)$ which are absolutely bandlimited to $[-B, B]$, whose energy mainly is concentrated within $[-T_c/2, T_c/2]$, and which accomplish a trade-off between synchronization accuracy on the one hand and tracking and acquisition robustness on the other hand, we solve the optimization problem given by (16), (17), (18), (19), and (20). In the following, the proposed systematic approach to optimum chip pulse shape design is applied within two examples. For both examples we restrict ourself to the case where $\varrho = \pi$, thus $B T_c = 1$ and $m \leq 5$ ($M = 5$). We will design either chip pulse shapes of even or odd symmetry. Whereas the $\psi_m(\varrho, t)$ are even for m even and odd for m odd we only need to solve for α_0, α_2, and α_4 for chip pulses of even symmetry and for α_1, α_3, and α_5 for chip pulses of odd symmetry. Thus, our optimization problem can be treated with very low complexity and we can be absolutely sure that we find the absolute optimum.

First the case of designing a GNSS signal for an empty band with $B = 10.23$ MHz is considered. There are no non-interoperable signals present in the same band, thus we will drop the constraint (20) for this case. The results of this example clearly show that this methodology can be applied to design a GNSS signal for example for C band or S band in order to accomplish the important trade-off in signal design between synchronization accuracy and acquisition and tracking robustness. New navigation signals in C band and S band are discussed recently [18]. The second example covers the case where a new GNSS signal shall be designed when already a non-interoperable signal is present in the same band and the SSC between the newly designed signal and this non-interoperable signal shall be limited. Exemplarily, we will

design a new signal for the E1/L1 band and the SSC between the newly designed signal and the GPS M Code signal shall be limited.

4.1. Example 1

We assume $B = 10.23$ MHz, $T_c = 1/B$, and $B_n = 1$ Hz. Whereas to achieve a smooth cut-off we choose $\gamma = 0.01$. As there are no non-interoperable signals present in the same band we drop the constraint (20). In order to also consider inter-chip-interference (ICI) we exemplarily use a Gold sequences of length 1023 as PN sequence. The designed chip pulse shapes $p(t)$ are convolved with this PN sequence and the performance of the signals is evaluated. In this example we only consider chip pulses of even symmetry.

Fig. 1 and Fig. 2 depict the derived chip pulse shapes in time and frequency domain respectively. The larger we choose κ the higher the time-sidelobes of the pulses become in time domain and the more energy is pushed to the edge of the band, as minimizing the CRLB is equivalent to maximizing the second moment of the power spectrum of the pulse $\int_{-\infty}^{\infty} f^2 \, |P(f)|^2 df$. This is bounded by the requirement that the energy of the optimum pulses shall be mainly concentrated within $[-T_c/2, T_c/2]$, which we set up in section 3. This requirement is justified as we desire to accomplish the trade-off between synchronization accuracy and tracking and acquisition robustness, which will be discussed next.
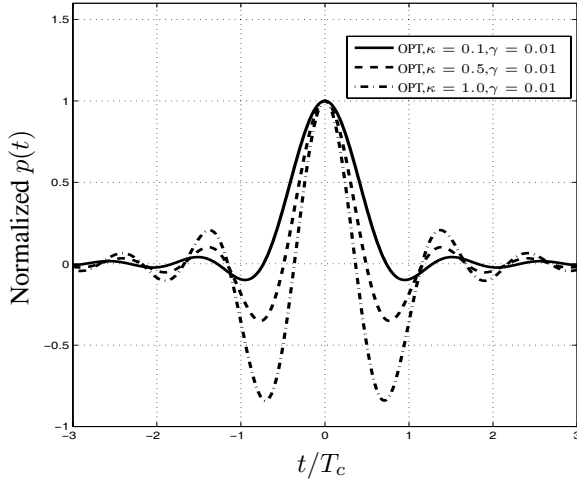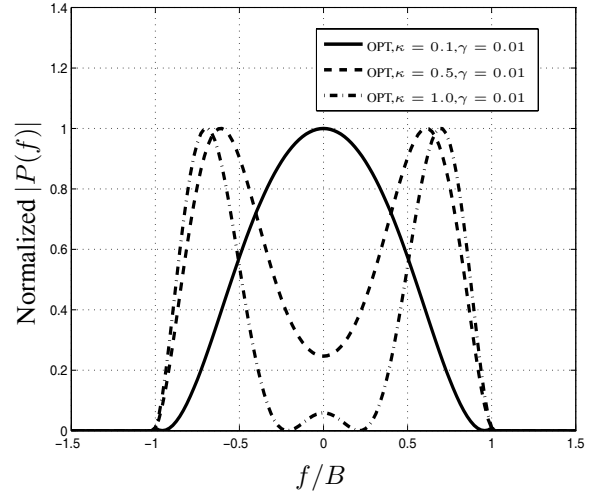

Fig. 2. Frequency domain

quantifies the trade-off between synchronization accuracy and acquisition and tracking robustness, as the higher the side extrema of $R(\varepsilon)$ become the less robust acquisition and tracking become. On the other hand the higher we choose κ the better the synchronization accuracy becomes. This can be clearly seen in Fig. 4 and Fig. 5 which depict the standard deviation of the estimation error of the time-delay and the loop S-curve.
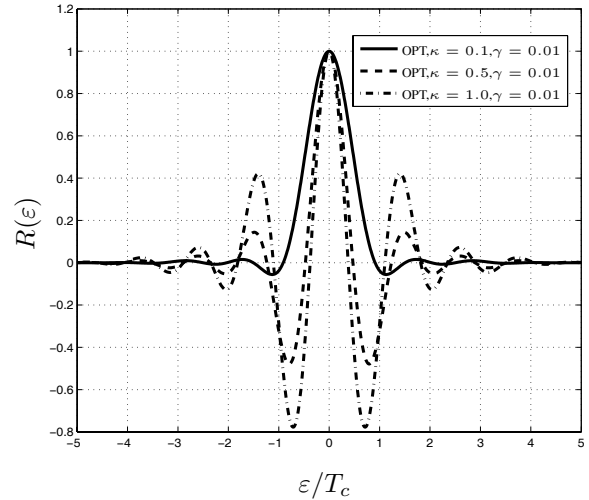

Fig. 1. Time domain

Fig. 3. Frequency domain

Fig. 3 shows the autocorrelation function $R(\varepsilon)$ for the chip pulse shapes. The higher we choose κ the higher the curvature $\frac{d^2 \, R(\varepsilon)}{d \, \varepsilon^2}$ at $\varepsilon = 0$ becomes, as discussed in section 3. However, the higher κ the higher the side extrema of $R(\varepsilon)$ become. Here, we clearly can observe that the parameter κ

Here, η denotes the tracking error in meters. For higher κ we notice that the S-curve shows additional stable look points with the same sign of the slope as in the lock point at $\eta = 0$. These additional stable lock points have to be avoided by appropriate techniques. Thus this results in less robust and
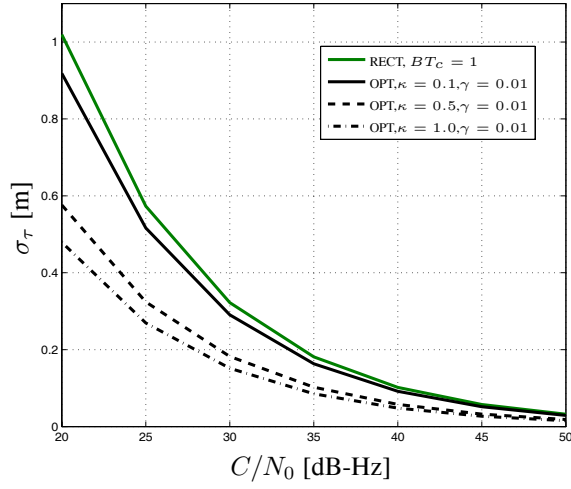
Fig. 4. Cramer-Rao lower bound for $B_n = 1$ Hz

Fig. 6. Time delay estimation error, multipath error envelope

more complex tracking. We compared the performance of the newly design chip pulse shapes to the performance of a bandlimited rectangular chip pulse with $B = 10.23$ MHz and $T_c = 1/B$. We consider the rectangular pulse as very robust, as the side extrema in its autocorrelation function are very low and there are no additional lock points in its loop S-curve.
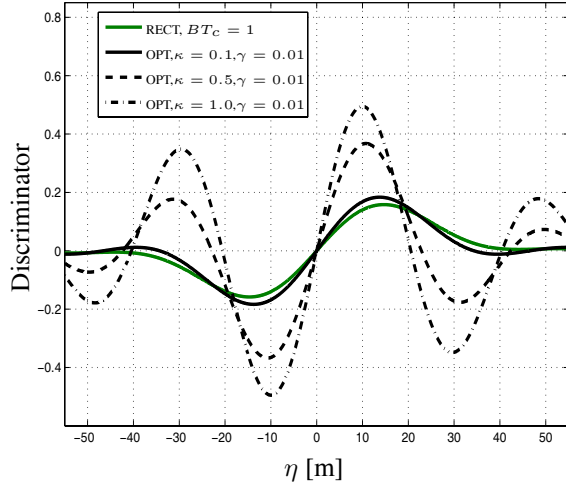

Fig. 5. Loop S-curve of an early-late discriminator using a Narrow correlator

Fig. 6 shows the time-delay estimation error bias for a two ray scenario, the multipath error envelope. The amplitude of the multipath is half of the amplitude of the line-of-sight signal (LOSS). The higher κ, the higher the multipath resistance of the signal becomes for short delayed multipath.
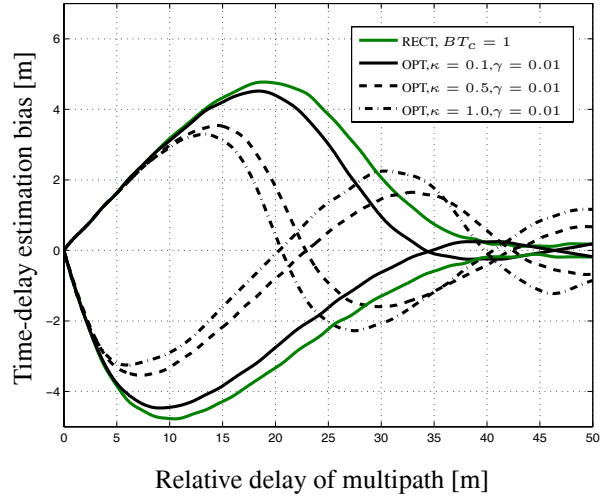
4.2. Example 2[*]

In this example we exemplarily design a new signal in the E1/L1 band centered at 1575.42 MHz. In order to achieve a smooth cut-off we choose $\gamma = 0.01$. Further we assume $\kappa = 1.0$, $B = 7.116$ MHz, and $T_c = 1/B$. We will consider pulses of even and odd symmetry. The constraint (20) is considered as a non-interoperable signal, the GPS M code is present in the same band. The SSC for (20) is chosen to -81.92 dB/Hz for a reference bandwidth $B_r = 16.368$ MHz. This SSC is equal to the SSC between the M code signal and the Galileo MBOC(6,1 1/11) signal for the reference bandwidth B_r.

Fig. 7 depicts the power spectrum density of the M code, the MBOC(6,1 1/11), and the resulting optimum signals applying chip pulse shapes of even and odd symmetry respectively. Fig. 8 shows the resulting optimum chip pulse shapes in time domain.

In Fig. 7 we can observe that the power of the resulting signals applying optimized chip pulse shapes of either even or odd symmetry is concentrated where the power spectrum density of the M code signal is low, in order to fulfill the constraint concerning the bounded SSC between the newly designed signals and the M code signal. Additionally, driven by the cost function of the presented approach, as much power of the new designed signals as possible is shifted towards the edge of the signal band ($B = 7.116$ MHz) in order to minimize the standard deviation of the time-delay estimation error. This example clearly demonstrates the flexibility and

[*]Nota bene: The presented examples to show how the presented method can be used in the practical case study of the E1/L1 band are not considered by Centre National d'Etudes Spatiales (CNES) as sufficiently spectrally separated from the GPS M code.
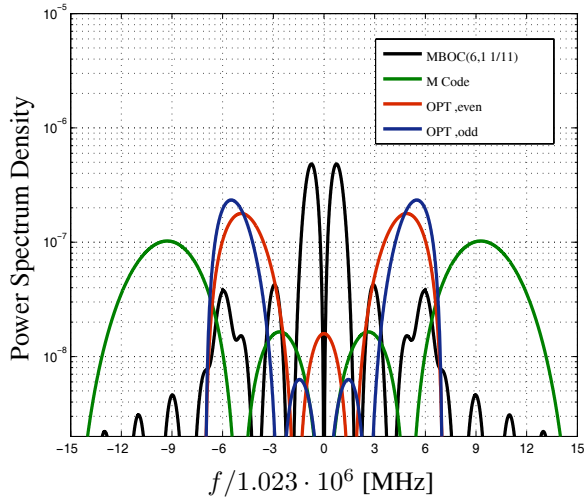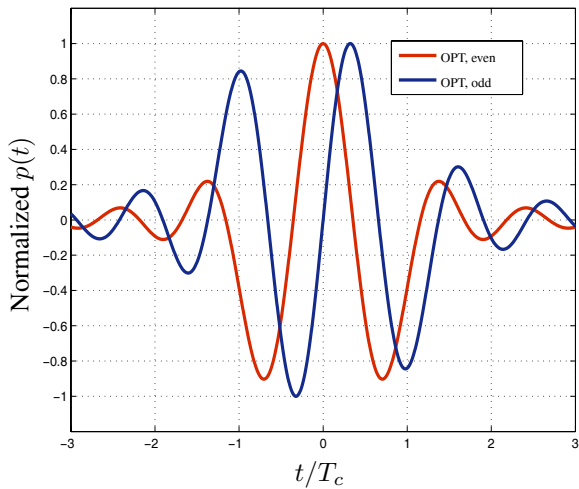
Fig. 7. Frequency domain

Fig. 9. Cramer-Rao lower bound for $B_n = 1$ Hz

Fig. 8. Time domain

Fig. 10. Time delay estimation error, multipath error envelope

capabilities of the presented systematic GNSS signal design approach. Fig. 9 shows the CRLB for $B_n = 1$ Hz and a reference bandwidth B_r for the MBOC(6,1 1/11) signal.

Fig. 10 depicts the multipath envelope, or the time-delay estimation bias for a two ray scenario. The amplitude of the multipath is half of the amplitude of the LOSS. For the MBOC(6,1 1/11) we used again the reference bandwidth B_r.

5. CONCLUSION

In this work we proposed a systematic approach to optimum chip pulse shape design for DS-CDMA systems. The proposed methodology makes it possible to formulate the problem of designing optimum chip pulse shapes $p(t)$ in terms of
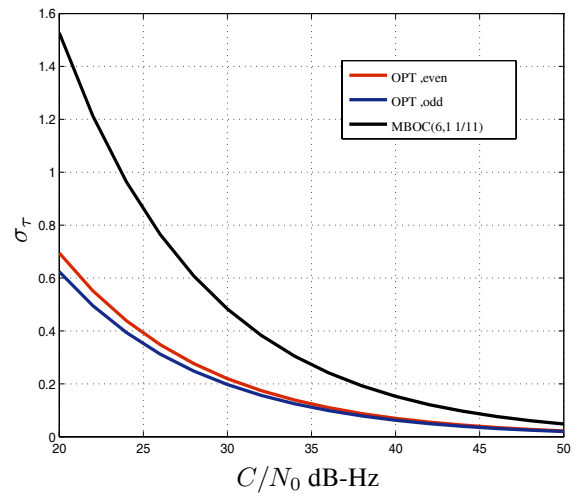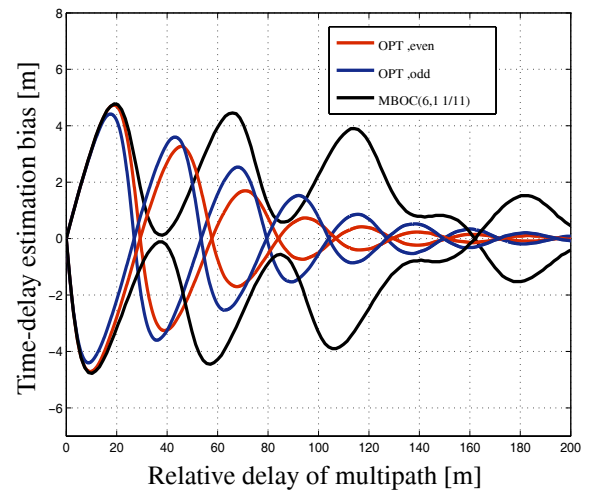
achieving a trade-off between synchronization accuracy and acquisition and tracking robustness, as an optimization problem. Thus, a systematic and general treatment of this problem was established. Several additional constraints which on the one hand quantify the trade-off between synchronization accuracy and acquisition and tracking robustness, and on the other hand which ensure practical signal generation and sufficient spectral separation were introduced to the optimization problem. The constraints which are introduced in this work seem sensible and also necessary, but more constraints can be easily defined. Thus, this approach can be expanded in a very efficient and flexible manner. Two examples were discussed in the section 4. The first example considered the case were a fixed bandwidth is given (assuming that spillover is not desirable here) and there are no non-interoperable signals present

in the defined signal band. This first example clearly demonstrates the capabilities of the proposed design approach. The important trade-off between synchronization accuracy and acquisition and tracking robustness was discussed. In the second example we designed a signal for which the SSC was limited with respect to a present non-interoperable signal in the same band. This second example underlines and extends the capabilities of the presented signal design approach for DS-CDMA signals. The presented methodology can be easily applied for GNSS signal design in C,S, and L band.

Future work may concern several topics, as signal performances with one or two bit receivers, signal optimization when spillover is possible, transformation of the primal formulation for bandlimited signals into the dual problem for time limited signals, signal optimization considering a two bit waveform to be interplexed with other waveforms, and an exploration of backward compatibility issues in L band.

6. REFERENCES

[1] S. W. Golomb and G. Gong, *Signal Design for Good Correlation*, Cambridge University Press, 2005.

[2] J. A. Avila-Rodriguez and et al., "The MBOC Modulation: The Final Touch to the Galileo Frequency and Signal Plan," in *Proceedings of the 20th Annual International Technical Meeting of the Satellite Division of the Institute of Navigation (ION)-Global Satellite Navigation System (GNSS)*, Fort Worth, TX, USA, September 2007.

[3] F. Antreich and J. A. Nossek, "On Chip Pulse Shape Design for Global Navigation Satellite Systems," in *Proceedings of the 2nd CNES-ESA Workshop on GNSS Signlas and Signal Processing, GNSS SIGNALS*, ESA-ESTEC, Noordwijk, The Netherlands, April 2007.

[4] J. A. Nossek and F. Antreich, "On chip pulse shape design for precise synchronization of DS-CDMA systems," *International Journal of Circuit Theory and Applications*, 2007,35(5-6):565-574.

[5] A. R. Pratt and J. I. R. Owen, "BOC Modulation Waveforms," in *Proceedings of the 16th Annual International Technical Meeting of the Satellite Division of the Institute of Navigation (ION) - Global Satellite Navigation System (GNSS)*, Portland, OR, USA, September 2003.

[6] D. Slepian and H. O. Pollak, "Prolate Spheroidal Wave Functions, Fourier Analysis and Uncertainty- I," *Bell Systems Technology Journal*, vol. 40, no. 1, 1961.

[7] H. J. Landau and H. O. Pollak, "Prolate Spheroidal Wave Functions, Fourier Analysis and Uncertainty- II," *Bell Systems Technology Journal*, vol. 40, no. 1, 1961.

[8] M. A. Landolsi, "Minimisation of Timing Jitter in CDMA Code Tracking," *IEEE Electronics Letters*, vol. 40, no. 21, 2004.

[9] M. A. Landolsi, "Perfromance Limits in DS-CDMA Timing Acquisition," *IEEE Transactions on Wireless Communications*, vol. 6, no. 9, 2007.

[10] T. Luo, S. Pasupathy, and E. S. Sousa, "Interference Control and Chip Waveform Design in Multirate DS-CDMA Communication Systems ," *IEEE Transactions on Wireless Communications*, vol. 1, no. 1, 2002.

[11] S. M. Kay, Ed., *Fundamentals of Statistical Signal Processing: Estimation Theory*, vol. 1, Prentice Hall PTR, 1993.

[12] D. R. White, "The Noise Bandwidth of Sampled Data Systems," *IEEE Transactions on Instrumentation and Measurement*, vol. 38, no. 6, 1989.

[13] R. D. Shelton and A. F. Adkins, "Noise Bandwidth of Common Filters," *IEEE Transactions on Communication Technology*, 1970.

[14] R. N. Barcewell, *The Fourier Transform and its Applications*, McGraw-Hill Book Company Inc., 1986.

[15] A. Papoulis, *The Fourier Integral and its Applications*, McGraw-Hill Book Company Inc., 1962.

[16] C. Flammer, *Spheroidal Wave Functions*, Stanford, CA: Stanford Univ. Press, 1957.

[17] S. Zhang and J. M. Jin, *Computation of Special Functions*, John Willey & Sons, Inc., 1996.

[18] J. A. Avila-Rodriguez and et al., "A Vision on new Frequencies, Signals and Concepts for Future GNSS Systems," in *Proceedings of the 20th Annual International Technical Meeting of the Satellite Division of the Institute of Navigation (ION)-Global Satellite Navigation System (GNSS)*, Fort Worth, TX, USA, September 2007.